

1 Genetic differentiation and intrinsic genomic features
2 explain variation in recombination hotspots among
3 cocoa tree populations

4 Enrique J. Schwarzkopf¹, Juan C. Motamayor², and Omar E. Cornejo^{1,*}

5 ¹School of Biological Sciences, Washington State University, 100 Dairy Road,
6 Pullman, WA 99164, USA

7 ²Universal Genetic Solutions, LLC

8 *Corresponding author: ocornejo@gmail.com

9 November 29, 2018

10 Abstract

11 Our study investigates the possible drivers of recombination hotspots in *Theobroma cacao*
12 using ten recently diverged populations. This constitutes the first time that recombination
13 rates from more than two populations of the same species have been compared, providing a
14 novel view of recombination at the population-divergence time-scale. For each population,
15 a fine-scale recombination map was generated using a method based on linkage disequi-
16 librium (LD). They revealed higher recombination rates in a domesticated population and
17 a population that has undergone a recent bottleneck. We address whether the pattern of
18 recombination rate variation along the chromosome is sensitive to the uncertainty in the per-
19 site estimates. We find that uncertainty, as assessed from the Markov chain Monte Carlo
20 iterations is orders of magnitude smaller than the scale of variation of the recombination
21 rates genome-wide. We inferred hotspots of recombination for each population and find that
22 the genomic locations of these hotspots correlate with genetic divergence between popula-
23 tions (F_{ST}). The large majority of inferred hotspots are not shared between populations
24 (55.5%). We developed novel randomization approaches for the generation of appropriate
25 null models to understand the association between hotspots of recombination and both DNA
26 sequence motifs and genomic features. Hotspot regions contained fewer known retroelement
27 sequences than expected, and were overrepresented near transcription start and termination
28 sites. Indicating that recombination hotspots are evolving in a way that is consistent with
29 genetic divergence, but are also preferentially driven to regions of the genome that contain
30 specific features.

31 Introduction

32 Genetic variation is fundamental for evolutionary forces like selection and genetic drift to
33 act. Selection and drift also contribute to a loss of variation, which means that they must act
34 in tandem with forces that maintain variation along the genome in order for populations to
35 continue evolving over prolonged periods of time. Selection and drift also contribute to a loss
36 of variation, which means that they must act in tandem with forces that maintain variation
37 along the genome in order for populations to continue evolving over prolonged periods of
38 time. Recombination's rearranging of genetic material onto different backgrounds generates
39 a larger set of haplotype combinations on which selection can act, reducing the magnitude
40 of Hill-Robertson interference (Felsenstein, 1974). Different regimes of recombination can
41 strongly influence how efficient selection is at purging deleterious mutations and increasing
42 the frequency of beneficial mutations in the population (Felsenstein, 1974).

43 Genome-wide fine-scale recombination maps can help elucidate the distribution of recom-
44 bination events along the genome (Myers et al., 2005; Auton et al., 2012; Brunshwig et al.,
45 2012; Paape et al., 2012; Choi et al., 2013; Hellsten et al., 2013; Singhal et al., 2015; Stevison
46 et al., 2016). These maps are constructed using methods that use the coalescent to leverage
47 current patterns of LD in order to estimate historical rates of recombination between sites
48 along the genome (Auton and McVean, 2007). Studies in a wide range of species have shown
49 that recombination rates are not uniform along the genome and general patterns of variation
50 have been described (Begun and Aquadro, 1992; Akhunov et al., 2003; Wu et al., 2003; An-
51 derson et al., 2004; McVean et al., 2004; Mézard, 2006; Kim et al., 2007; Gore et al., 2009;
52 Schnable et al., 2009; Branca et al., 2011; Paape et al., 2012). One of these patterns is the
53 reduced recombination rate in centromeric regions of the chromosomes and the progressive
54 increase of recombination rates as the physical distance to telomeres decreases (Begun and
55 Aquadro, 1992; Akhunov et al., 2003; Wu et al., 2003; Anderson et al., 2004; Gore et al., 2009;

56 Schnable et al., 2009). Another, perhaps more interesting pattern that has been observed is
57 regions with unusually high rates of recombination spread throughout chromosomes: recom-
58 bination hotspots (McVean et al., 2004; Brunschwig et al., 2012; Paape et al., 2012; Hellsten
59 et al., 2013; Stevison et al., 2016; Shanfelter et al., 2018). The importance of recombination
60 hotspots lies in their ability to shuffle genetic variation at higher rates than the rest of the
61 genome, profoundly impacting the dynamics of selection for or against specific mutations
62 (Felsenstein, 1974).

63 A variety of genomic features have been identified as being associated with regions of
64 high recombination. In *Arabidopsis thaliana*, *Taeniopygia guttata*, *Poephila acuticauda*, and
65 humans, hotspots have been linked to transcriptional start sites (TSSs) and transcriptional
66 termination sites (TTSs) (Myers et al., 2005; Choi et al., 2013; Singhal et al., 2015). In
67 *Mimulus guttatus* hotspots were found to be associated with CpG islands (short segments of
68 cytosine and guanine rich DNA, associated with promoter regions) (Hellsten et al., 2013).
69 These patterns point to recombination occurring frequently near, but not within coding
70 regions. The formation of chiasmata is important for the proper disjunction of chromosomes
71 during meiosis (Martinez-perez et al., 2008), but repeated double-strand breaks can lead to
72 an increased mutation rate (Rodgers and Mcvey, 2015). In coding regions in particular this
73 excess mutation rate can have a high evolutionary cost, due to the likelihood of deleterious
74 mutations arising being higher than that of beneficial ones (Haldane, 1937; Crow, 1970;
75 Wloch et al., 2001; Sanjuán et al., 2004; Eyre-Walker and Keightley, 2007). Recombination
76 hotspots have also been found to be correlated with particular DNA sequence motifs. In
77 some mammals, including *Mus musculus* (Brunschwig et al., 2012) and apes (Auton et al.,
78 2012; Stevison et al., 2016) binding sites for PRDM9, a histone trimethylase with a DNA
79 zinc-finger binding domain, have been found to correlate with recombination hotspots. In
80 *Arabidopsis*, proteins have been identified that limit overall recombination rate, leading to
81 an increased recombination rate genome-wide in mutants (Fernandes et al., 2018). However,

82 these proteins have not been shown to direct recombination to particular regions, and are
83 therefore not expected to affect the location of recombination hotspots.

84 Recent work on recombination in apes (Stevison et al., 2016) found little correlation
85 of recombination rates in orthologous hotspot regions when looking between species, but a
86 strong correlation when comparing between two populations of the same species. This sug-
87 gests that recombination hotspots are potentially changing in ways that match demographic
88 patterns, differentiating at a similar rate as genomic sequences. The identification of ten
89 recently diverged populations of the cocoa tree, *Theobroma cacao* (Motamayor et al., 2008;
90 Cornejo et al., 2018) can be leveraged to study short-term drivers of recombination hotspots.
91 These ten populations originate from different regions of South and Central America, and
92 include one fully domesticated species (Criollo), used in the production of fine chocolate, and
93 nine wilder, more resilient species which generate higher cocoa yield than the Criollo variety
94 (fig. 1) (Motamayor et al., 2008; Henderson et al., 2007; Cornejo et al., 2018). These ten
95 populations have been shown to be highly differentiated and the history of diversification has
96 been recently confirmed using genomic data (Cornejo et al., 2018). Comparing the locations
97 of hotspots between these ten populations of *T. cacao* can contribute to the understanding
98 of hotspot turnover in short periods of time among highly differentiated populations. These
99 comparisons also contribute to our understanding of how demographics impact the turnover
100 of recombination hotspot locations.

101 Fine-scale, LD-based recombination maps have been constructed for a number of plant
102 models (Paape et al., 2012; Choi et al., 2013; Hellsten et al., 2013), and in all of them a
103 variety of correlates of recombination rate have been identified. Unlike these model plants
104 with short generation times, *T. cacao* is a perennial woody plant with a five-year genera-
105 tion time (Henderson et al., 2007). Studying recombination in *T. cacao* presents particular
106 difficulties due to its long generation time, making it difficult to directly measure rates of
107 recombination. However, linkage-based methods allow for the estimation of historic recombi-

108 nation rates (Auton and McVean, 2007), facilitating the study of historical recombination in
109 *T. cacao*. Theoretical studies have shown that population structure can generate artificially
110 inflated measures of LD (Ohta, 1982; Li and Nei, 1974), which would be detrimental to our
111 estimates of recombination. For this reason recombination maps were constructed indepen-
112 dently for each population. In contrast to previous studies, which have focused primarily on
113 recombination rates, this study attempts to describe the relationship between recombination
114 hotspots and a variety of factors.

115 A series of questions were addressed in this work: (i) How are recombination rates dis-
116 tributed within 10 highly differentiated populations of *T. cacao*, and how do they compare
117 to each other? (ii) How are hotspots distributed along the genome of each of the ten popula-
118 tions of *T. cacao*, and can these distributions be explained by patterns of population genetic
119 differentiation? (iii) Are there identifiable DNA sequence motifs that are associated with the
120 location of recombination hotspots along the *T. cacao* genome? (iv) Are there genomic fea-
121 tures (e.g. TSSs, TTSs, exons, introns) consistently associated with recombination hotspot
122 locations across *T. cacao* populations?

123 In order to address these questions, we used an LD-based method to estimate recombina-
124 tion rates, since *T. cacao*'s generation time and sheer size make performing a large number of
125 backcrosses unfeasible. We used the estimated recombination rates in a maximum likelihood
126 statistical framework to infer the location of recombination hotspots. Then we compared
127 the location of hotspots across populations and found evidence that, while hotspots gener-
128 ally follow patterns of genetic differentiation, their turnover rate is faster than the rate of
129 divergence. We used resampling schemes to generate null assumptions for the content of
130 known DNA sequence motifs in ubiquitous recombination hotspots, as well as the overlap
131 of population recombination hotspots with genomic traits. The resampling schemes used to
132 identify these associations are novel in the context of this work and were designed to take
133 into account the size and distribution of elements in the genome. Our findings suggest that

134 recombination hotspot locations generally follow patterns of diversification between popula-
135 tions, while also having a strong tendency to occur close to TSSs and TTSs. Moreover, we
136 find a strong negative association between the occurrence of recombination hotspots and the
137 presence of retroelements.

138

139 Results

140 *Comparing recombination rates between populations*

141

142 Populations show a mean recombination rate r/kb between 2.1×10^{-5} and 5.25×10^{-3}
143 (table 1), with a long-right-tailed distribution (fig. 3). The extreme recombination rate
144 values affect the mean, driving it to values consistently higher than the median. The pattern
145 of recombination rates along the genome varied between populations, as can be seen in the
146 comparison of the Nanay and Purus third chromosome (fig. 4). The median 95% probability
147 interval for recombination rate across the genome for each population was found to be several
148 orders of magnitude larger than the uncertainty per site, estimated as the median 95%
149 Credibility Interval of the trace for each position in the genome for that population (table
150 6).

151 Overall, the recombination rate for most of the populations was higher than estimated
152 mutation rates for multicellular eukaryotes of 10^{-6} changes per kb per generation (Lynch,
153 2010; Exposito-Alonso et al., 2018) (table 1). Two populations, Guianna and Criollo, were
154 notable exceptions, having higher average recombination rates than the other populations
155 by one and two orders of magnitude respectively. Guianna and Criollo also had a lower
156 effective population size (N_e) (Cornejo et al., 2018) by one and two orders of magnitude
157 respectively. However, there was no significant linear trend between mean N_e and r/kb

158 ($p=0.09045$), indicating that, for a high enough N_e , the ability to detect recombination
159 events is not dictated by the effective population size. When Criollo and Guianna were
160 excluded, the relationship was also not present ($p = 0.6544$). When all populations were
161 included, the inbreeding coefficient (F) showed no significant linear association with mean
162 r/kb ($p = 0.3361$). The average recombination rate per population was transformed from
163 r/kb to cM/Mb (table 1). The average cM/Mb was 4.6×10^{-04} .

164 In order to compare the average recombination rates of the different populations, a
165 Kruskal-Wallis test was performed for every pair of populations. The only pair of popu-
166 lations that did not show a significant difference in mean recombination rate was the pair
167 of Nacional and Nanay ($p = 0.3$). All other pairwise comparisons were highly significant
168 ($p < 2 \times 10^{16}$).

169

170 *Comparing recombination hotspot locations between populations*

171

172 The majority (55.5%) of hotspots identified were not shared between populations. The
173 25 most numerous sets of hotspots are represented in fig. 6. The nine largest of these are sets
174 of hotspots unique to a single population. The hotspots unique to the remaining population
175 (Criollo) formed the eleventh largest set.

176 The recombination rate in hotspot regions for nine of the populations was on average be-
177 tween 22 and 237% higher than the average recombination rate of the genome. The exception
178 was Guianna, which only showed an approximately 1% increase in average recombination
179 rate in hotspot regions when compared to that of the non-hotspot regions.

180 Despite the majority of hotspots not being shared between populations, pairwise Fisher's
181 exact tests between populations indicated significantly more overlap than expected (if hotspots
182 were randomly distributed along the genome) between hotspots for most pairs of popula-
183 tions (table 2). There were three comparisons that did not show significantly more overlap

184 than expected: Amelonado-Nacional, Amelonado-Purus, and Criollo-Nacional. A Mantel
185 test comparing distances between populations based on shared hotspots and F_{ST} values be-
186 tween populations resulted in a significant correlation between them ($r = 0.66$, $p = 0.002$).
187 The correlation between eigenvectors from a correlation matrix and those of the genetic
188 covariance matrix were also explored. When all populations were included, we found that
189 the first eigenvector from the genetic covariance matrix was not significantly correlated with
190 the first eigenvector from the hotspot correlation matrix ($p = 0.7055$), but the second ge-
191 netic eigenvector was ($p = 0.009007$, $r = 0.7711638$). However, the first eigenvector of the
192 genetic covariance matrix captured the difference between the Criollo population (the only
193 domesticated variety) and the rest of the populations. The second eigenvector explains most
194 of the natural differentiation across populations (Cornejo et al., 2018). For that reason, we
195 decided to exclude Criollo and repeat the analysis. We found that the first eigenvector from
196 the correlation matrix constructed from shared hotspot information was not significantly
197 correlated with either of the first two eigenvectors of the genetic covariance matrix when
198 Criollo was excluded (eigenvector 1: $p = 0.1314$, eigenvector2: $p = 0.3376$).

199 To study the effects of demographic history more closely, shared hotspots were converted
200 to dimensions of a multiple correspondence analysis and modeled along a previously con-
201 structed drift tree (Cornejo et al., 2018). The model assuming an OU process (stabilizing
202 selection) is consistent with a higher trait maintenance than the model assuming Brownian
203 motion (drift). Modeling the dimension as a Brownian motion was a better fit (AIC=79.4)
204 than modeling it as an Ornstein-Uhlenbeck (OU) process (AIC=81.4), which is consistent
205 with the small number of hotspots shared between populations.

206

207 *Identifying DNA sequence motifs associated with the locations of recombination hotspots*

208

209 RepeatMasker was used to analyze the set of recombination hotspots that were present

210 in at least eight *T. cacao* populations (17 total hotspots), as well as the consensus set
211 of recombination hotspots, and the reference genome. In order to determine whether a
212 particular set of DNA sequence repeats was overrepresented in the regions of ubiquitous
213 recombination hotspots, the percentage of DNA sequence that was identified as potentially
214 being from retroelements or DNA transposon was compared to an empirical distribution.
215 The percentage of observations from the distribution which were greater than the observed
216 are reported in table 3. While retroelements were found to be underrepresented in the ubiq-
217 uitous hotspots, DNA transposons were marginally overrepresented.

218

219 *Identifying genomic features associated with the location of recombination hotspots*

220

221 An overrepresentation of recombination hotspots was found in all ten of the populations
222 at transcriptional start sites (TSSs) and transcriptional termination sites (TTSs)(table 4).
223 The level of overrepresentation of hotspots in particular regions was compared to a null ex-
224 pectation based on simulations of hotspots of the same size as the ones detected distributed
225 randomly along chromosomes. For all populations, all 1000 simulations showed a lower pro-
226 portion of overlap with TSSs and TTSs than the observed overlap. In the case of exons and
227 introns, seven populations (Contamana, Criollo, Iquitos, Maranon, Nacional, Nanay, Purus)
228 had an observed value that was lower than all, or almost all (Purus for exons), simulations.
229 Three of the remaining four populations (Amelonado, Curaray, and Nanay) had no clear
230 trend in either direction (table 2). The final population (Guianna) showed an overpresen-
231 tation of hotspots in both exons and introns.

232

233 Discussion

234 Understanding how recombination rates vary between recently diverged populations is an
235 important step toward disentangling the role of recombination in genetic differentiation.
236 This set of *T. cacao* populations presents a unique opportunity to observe recombination
237 in long-established, non-domesticated populations, as well as a recently established non-
238 domesticated population (Guianna) and a domesticated population (Criollo) (Cornejo et al.,
239 2018; Bartley, 2005). This model has allowed us to explore divergence patterns of recombina-
240 tion hotspot at a scale bellow that of species divergence. Our results point to a conservation
241 of hotspots between populations that generally mirrors the patterns of genetic differentiation
242 between populations. However, we find that the correlation between genetic differentiation
243 and shared hotspots does not fully explain the observed hotspots, in part due to the ma-
244 jority of hotspots being found in a single population. We find that TSSs and TTSs are
245 strongly associated with recombination hotspots in all populations, which is consistent with
246 previous findings in plants (Paape et al., 2012; Choi et al., 2013; Hellsten et al., 2013). This
247 factor seems to play an important role in determining the location of novel hotspots. Fi-
248 nally, hotspots that are shared by at least eight populations appear to be associated with
249 DNA transposons, pointing to a potential mechanism for the maintenance of recombination
250 hotspots at the population-divergence time-scale.

251

252 *Comparing recombination rates between populations*

253

254 We found that the eight long-established, non-domesticated *T. cacao* populations show a
255 recombination rate (r/kb) lower than multicellular eukaryotic mutation rates (table 1), while
256 the other two populations (Criollo and Guianna) show unusually high average recombination
257 rates in comparison. For all populations, the mean recombination rate was found to be lower

258 than the median. This is consistent with high rate outlier values; an expected result in the
259 presence of recombination hotspots. Using the effective population size for *Medicago trun-*
260 *catula* from Siol et al. (2007) and the estimate of ρ from Paape et al. (2012), we calculated
261 r/kb ($= 4 \times 10^{-3}$) and found that it was comparable with the rate found for the Criollo
262 population (table 1). We also calculated the median recombination rate in cM/Mb for each
263 chromosome using the Kosambi mapping function (Kosambi, 1943) over non-overlapping,
264 100 SNP windows. The average cM/Mb for all populations was 4.6×10^{-04} , which is lower
265 than has been measured for any Malvale (Kundu et al., 2015), but not as low as the lowest
266 measured for conifers (Chen et al., 2010; Stapley et al., 2017). Average recombination rates
267 in cM/Mb varied between populations from Amelonado (4.04×10^{-06}) to Criollo (3.91×10^{-03}).
268 Previous work (Cornejo et al., 2018) has shown that Criollo is the only population showing
269 a strong signature of domestication, as revealed by much higher drift than that observed
270 for other populations. Domestication has been observed to increase recombination rates,
271 particularly in plants (Ross-Ibarra, 2004), and is a possible explanation for the higher re-
272 combination rate observed for the Criollo population. The high recombination rate observed
273 in Guianna can be explained in a similar way; while Guianna does not show a strong signa-
274 ture of domestication, it is the most recently established population (Bartley, 2005), and it
275 has also undergone a recent bottleneck (Cornejo et al., 2018). It's possible that the Guianna
276 population is undergoing the initial stages of domestication and its increased recombination
277 is an early indicator of this. It is possible that the high recombination rates estimated for
278 Criollo and Guianna can be explained by biases in estimation caused by errors associated
279 to small samples or low genetic variation; yet, the recombination rates for Amelonado (an-
280 other population with low variation) or Purus (a population with small sample size) did not
281 present this problem. Analyses exploring mutations of putative recombination suppression
282 genes (Fernandes et al., 2018) could help disentangle the nature of this extreme variation in
283 recombination rate in the Criollo and Guianna populations.

284 Despite recombination rates for eight of the ten populations being of the same order
285 of magnitude, pairwise comparisons of average rates indicated that most populations have
286 a significantly different rate of recombination from the others. The only exception were
287 Nacional and Nanay whose average rates were not significantly different from each other.
288 These two populations, however, are not more closely related to each other than they are
289 to other populations, based on sequence divergence (Cornejo et al., 2018). We interpret
290 this result as suggestive that their similarity is not due to genetic similarity, but some other
291 factors, e.g. epigenetics.

292 The likelihood of detecting Hotspots of recombination in the genome will likely be af-
293 fected by the amount uncertainty in the estimates of recombination site-wise and region-wise.
294 Yet, we have been unable to identify any study where the magnitude of the uncertainty in
295 the estimates of recombination are assessed to address this issue. We have performed careful
296 comparisons and assessed the magnitude of the uncertainty in the estimation of recombi-
297 nation rates to show that this uncertainty is several orders of magnitude smaller than the
298 variation in recombination rates across the genome (table 6). If the length of the chains had
299 been maintained at 40MM generations, this would have increased the uncertainty in local
300 estimates making our assessment of rate variation along the genome more challenging.

301

302 *Comparing recombination hotspot locations between populations*

303

304 Similarly to recombination rates, the location of recombination hotspots can be very
305 informative to questions of divergence between populations. Understanding the pattern and
306 rate of change of recombination hotspots at the population level can elucidate their role in
307 shaping genome architecture, impacting how effectively selection operates (Felsenstein, 1974).
308 We found that a large proportion (55.5%) of hotspots are unique to a single population, which
309 can be seen as an indicator that the turnover rate for hotspots is faster than the time it took

310 the 10 populations to diverge. This variability of hotspot location between populations
311 points to demographic history not being the main driver of recombination hotspot location.
312 However, the hotspots tend to appear in similar regions, as demonstrated by the Fisher's
313 exact tests (table 2). This dichotomy can be explained by considering that the proportion
314 of the genome occupied by recombination hotspots is very low, so even a small proportion of
315 hotspots from two different populations being in the same region is enough for the Fisher's
316 exact test to recognize them as significantly similar. This small but significant similarity
317 can occur by recombination being limited in its possible positioning along the genome, but
318 not to the point of forcing hotspots to occur consistently in the same locations, and thus
319 maintaining some level of stochasticity.

320 Given the significant proportion of overlapping hotspots between populations, it was still
321 important to explore whether the similarities can be explained by shared genetic history. If
322 demographic history explained the evolution of hotspot location, it would be expected that
323 more closely related populations would have a higher percent of overlapped hotspots. A
324 significant relationship was found between population differentiation (F_{ST}) and the differ-
325 entiation between populations based on shared hotspots (Mantel test, $r = 0.66$, $p = 0.002$).
326 The comparison between the hotspot correlation matrix and the genetic covariance matrix
327 supports what was found when comparing the hotspot correlation matrix to the F_{ST} matrix.
328 One caveat is that the first genetic eigenvector, which separated Criollo from the other pop-
329 ulations, was not correlated with the first hotspot correlation eigenvector, indicating that
330 Criollo's domestication generated a genetic pattern that deviates from the pattern of shared
331 hotspots. This indicates that, to some extent, the genetic differentiation and the location
332 of hotspots are mirroring each other, which could be due to recombination hotspots being a
333 product of the shared history between the populations. However, since recombination rates
334 were estimated using a coalescent-based method, we expect historical relationships to be
335 represented in our findings. We also transformed the information of hotspot overlap to allow

336 for the modeling of hotspots as traits along a population tree. Our results, showing that
337 a Brownian motion model (AIC=79.4) better fits the data than a model with stabilizing
338 selection Ornstein-Uhlenbeck model (AIC=81.4), suggests in first principle that drift alone
339 could explain the evolution of the location of recombination hotspots. However, the absolute
340 number of hotspots that are shared among populations indicates that demographic history
341 alone is insufficient to explain the evolution of recombination hotspots in this species. Pre-
342 vious studies looking at apes and finches have explored recombination hotspots in multiple
343 species and as many as two populations of the same species (Singhal et al., 2015; Stevison
344 et al., 2016; Shanfelter et al., 2018), but this study is the first to compare more than two
345 populations of the same species at once. The increased number of populations allows us
346 to analyze the relationship between population genetic processes and recombination. Our
347 results suggest that the pattern of gains and losses of recombination hotspots can be very
348 dynamic and the landscape of recombination changes rapidly during the process of diver-
349 sification within a species. This dynamism can have a tremendous impact on the adaptive
350 dynamics of a species, and it should be taken into account, considering that theoretical stud-
351 ies tend to assume that recombination rates are constant during the evolution of populations
352 (Hudson and Kaplan, 1988; Donnelly and Kurtz, 1999).

353 One conclusion that follows from these results is that, while shared recombination hotspots
354 can to some extent be explained by patterns of genetic differentiation, some of the sharing
355 can simply be due to a tendency for hotspots to arise in similar locations. It has been ob-
356 served in other organisms that hotspots of recombination are frequently associated to specific
357 genomic features (including TSSs and TTSs) (Auton et al., 2013; Choi et al., 2013; Hellsten
358 et al., 2013; Myers et al., 2005; Singhal et al., 2015) or DNA sequence motifs (Auton et al.,
359 2012; Brunshwig et al., 2012; Stevison et al., 2016). These factors can affect the landscape
360 of recombination, generating the patterns of shared hotspot locations between populations
361 that we are observing in *T. cacao*.

362

363 *Identifying DNA sequence motifs associated with the locations of recombination hotspots*

364

365 The analysis of 17 hotspots shared between at least eight populations of *T. cacao* found
366 an underrepresentation of retroelements and a marginal overrepresentation of DNA trans-
367 posons when compared to the entire genome. These results are not entirely surprising as
368 it has been already suggested that transposable elements (TEs) tend to be enriched in ar-
369 eas of low recombination in *Drosophila* as a consequence of selection against TEs (Rizzon
370 et al., 2002). The marginal over-representation of DNA transposons in the most conserved
371 recombination hotspot is unexpected, given that all previous observations have shown a
372 reduced representation of mobile elements in areas with high recombination rate (Rizzon
373 et al., 2002). It's possible that DNA transposons are, at least in part, responsible for the
374 maintenance of recombination hotspots as populations diverge, from which we expect that
375 site-directed recombination is more frequent in these locations of the genome. However, the
376 low percentage of these sequences observed in the set of all hotspots (table 3) indicates that
377 these sequences only have a small effect on the maintenance of hotspots. It has been observed
378 in humans that short DNA motifs enriched for repeat sequences determine the location of 40
379 per cent of hotspots enriched for recurrent non-allelic homologous recombination (Mcvean,
380 2010). One potential explanation that for why natural selection does not eliminate hotspots
381 in these regions is the possibility that these regions don't produce a large enough mutational
382 load for natural selection to remove them from the population (Mcvean, 2010).

383

384 *Identifying genomic features associated with the location of recombination hotspots*

385

386 For all ten populations, an overrepresentation of hotspots was found in the areas imme-
387 diately preceding and following transcribed regions of the chromosome. This matches the

388 findings of previous studies in *Arabidopsis thaliana* (Choi et al., 2013), *Taenipygia guttata*
389 and *Poephila acuticauda* (Singhal et al., 2015), and humans (Myers et al., 2005). The most
390 likely explanation is that recombination events within genes are selected against. The ra-
391 tionale is that a recombinant chromosome that is split in the middle of a coding region will
392 have a higher risk of being inviable, and therefore not represented in the current set of chro-
393 mosomes for its population. Recombination occurring in transcription start and stop sites,
394 on the other hand, does a much better job at breaking up haplotypes, while preserving the
395 functionality of coding regions. This rationale is supported by previous findings of increased
396 recombination rates in these regions (Choi et al., 2013). It's also supported by results from
397 PRDM9 knock-out *Mus musculus*, which has shown a reversion to hotspots located near
398 TSSs (Brick Kevin et al., 2012). The enrichment of *T. cacao* hotspots in TSSs and TTSs
399 is thus a reasonable result given that zinc-finger binding motifs and potential modifiers like
400 PRDM9 have not been identified in the species.

401

402 *Implications for the evolutionary history of T. cacao*

403

404 Overall, our results show a large consistent pattern where recombination rates in *T. ca-*
405 *cao* are of the same magnitude as mutation rates, but show a high diversity in location
406 and number of hotspots of recombination that cannot be explained solely by the process of
407 diversification of the populations. In fact, the results are indicative that the turnover rate of
408 hotspots is faster than the process of divergence among populations. A potential hypothesis
409 that could explain the rapid turnover of hotspots of recombination and the relative differ-
410 ences in recombination among populations is that epigenetic changes control the turnover of
411 recombination in plants. This hypothesis is not unreasonable given the recent observation
412 of epigenetic control of recombination in plants (Yelina et al., 2015). Further theoretical
413 and simulation work should be done in order to better understand the implications of the

414 rapidly changing recombination hotspots in adaptive dynamics. We also show that there is
415 an overall underrepresentation of hotspots in exons and introns for most populations, which
416 is consistent with purifying selection acting against changes that could result in disruptions
417 of gene function. On the other hand, we observed an overrepresentation of hotspots in TTSs
418 and TSSs for all ten populations. This could impact the maintenance and spread of benefi-
419 cial traits in the population by shuffling allelic variants of genes without causing disruption
420 of their function. We hypothesize that the enrichment of hotspots of recombination in TTSs
421 and TSSs can have an important impact in the spread of beneficial mutations across different
422 genomic backgrounds; increasing the rate of adaptation to selective pressures (e.g. selection
423 for improved pathogen response).

424

425 **Materials and Methods**

426 *Comparing recombination rates between populations*

427

428 Sequence data were downloaded from the Cacao Genome Database and NCBI (Accession
429 PRJNA488484), including the reference sequence for each chromosome and the full genome
430 annotation (*Theobroma cacao* cv. Matina 1-6 v1.1)(Motamayor et al., 2013). Processing
431 was done using the pipeline from (Cornejo et al., 2018) available at the github repository
432 *oeco28/Cacao_Genomics*. Full genome data was used from a total of 73 individuals across
433 10 populations (Cornejo et al., 2018): Criollo (N = 4, #SNPs = 309,818), Curaray (N =
434 5, #SNPs = 1,106,871), Contamana (N = 9, #SNPs = 2,097,618), Amelonado (N = 11,
435 #SNPs = 373,789), Marañon (N = 14, #SNPs = 1,783,226), Guianna (N = 9, #SNPs =
436 770,729), Iquitos (N = 7, #SNPs = 1,575,711), Purus (N = 6, #SNPs = 1,184,181), Nanay
437 (N = 10, #SNPs = 830,885), and Nacional (N = 4, #SNPs = 718,099). VCFTools (Danecek

438 Petr et al., 2011) was used to remove all singletons and doubletons. Only bi-allelic single
439 nucleotide polymorphisms (SNPs) were retained and were exported in LDhat format.

440 In order to estimate recombination rates we used the *interval* routine of LDhat (Auton
441 and McVean, 2007), a program that implements coalescent resampling methods to estimate
442 historical recombination rates from SNP data. To reduce computation time, each chromo-
443 some was split into windows, each containing 2000 SNPs. To counteract the overestimation
444 of recombination rate produced at the ends of the windows, an overlap of 500 SNPs was left
445 between consecutive windows. The final window for each chromosome did not always match
446 the general scheme, so the final 2000 SNPs were taken (making the overlap with the second
447 to last window variable, but never less than 500 SNPs) (fig. 2). Once these windows were
448 generated, LDhat was run over each window with 100 million iterations, sampling every 10
449 thousand iterations (10,000 total points sampled), with a block penalty of 5. Lookup tables
450 with a grid of 100 points, a population mutation rate parameter (θ) of 0.1 and a number
451 of sequences (n) of 50 were used for all populations. The first 50 million iterations were
452 discarded as burn-in. Once recombination rates were calculated, 250 positions were cut off
453 from both windows involved in each overlap, so that the estimates for the first half of the
454 overlap was taken from the end of the preceding window and the estimates for the second
455 half of the overlap were taken from the beginning of the following window. The final overlap
456 in each chromosome was split in order to take only 250 SNPs from the second to last window,
457 regardless of the remaining size of the last window. The remaining rate estimates were then
458 merged in order to obtain the recombination rates for the entire chromosome. This was done
459 for each chromosome of each population.

460 The estimation of recombination rates with LDhat is approximated using a sampling
461 scheme with a Markov Chain Monte Carlo (MCMC) algorithm as implemented in the *interval*
462 routine. The inference of recombination rates is the result of the integration of estimated
463 parameter values across iterations with the routine *stats*. In the majority of recent studies

464 where LDhat or LDhelmet are used (Myers et al., 2005; Auton et al., 2012; Brunshwig et al.,
465 2012; Paape et al., 2012; Auton et al., 2013; Choi et al., 2013; Singhal et al., 2015; Stevison
466 et al., 2016), whether there is convergence of the Markov chains has not been explicitly
467 investigated. One study that we're aware of has used simulations to asses whether their
468 small sample size affected their ability to obtain reliable estimates of recombination using
469 LDhelmet (Booker et al., 2017), but did not assess the uncertainty of the estimates from
470 the MCMC process itself. We argue that evaluation of convergence is important to assess
471 the confidence in the estimated reported values, especially if there is interest in analyzing
472 the differences in recombination rate along the genome. Visual inspection of pilot runs of
473 the analysis demonstrated that convergence was not achieved after running 40M iterations,
474 which is why the length of the chains was increased to 100M iterations. Additionally we
475 explored the uncertainty in the estimates of recombination site-wise by integrating over the
476 trace of the estimates for recombination rate to infer the 95% Credibility Interval. We then
477 estimated the 95% of recombination estimates range across all sites in the genome to have
478 an overall measure of uncertainty that we compared to the median 95% Credibility Interval
479 for the trace of each position.

480 In order to compare recombination rates, the effective population size (N_e) calculated for
481 each population (Cornejo et al., 2018) was used to convert rates in $N_e r/kb$ to r/kb . Differ-
482 ences in the mean genome-wide recombination rate between populations were then tested
483 using the Kruskal-Wallis test, using the `kruskal.test` function from the `stats` package in R
484 (R Core Team, 2018). There were 45 comparisons, making the Bonferroni correction cutoff
485 value: $\alpha = 0.0011$. To transform per population recombination rates from r/kb to cM/Mb ,
486 we divided each chromosome into windows of 100 SNPs and used the Kosambi mapping func-
487 tion (Kosambi, 1943). The median for the windows of a chromosome was then calculated,
488 and the average of each population's chromosomes was taken as that population's average
489 recombination rate in cM/Mb .

490

491 *Comparing recombination hotspot locations between populations*

492

493 Recombination hotspots were estimated with LDhot (Auton and McVean, 2007), a likelihood-
494 based program that tests whether a single distribution model or a two distribution model
495 better explains the observed recombination rates in 1 kb sliding windows (default), for each
496 chromosome. Each chromosome was run in its entirety, with the number of simulations
497 (nsims) set to 1000. The resulting potential hotspots were refined by an alpha of 0.001, and
498 overlapping hotspots were merged.

499 To determine the set of consensus hotspots, the hotspots from all populations were
500 merged. Two hotspots from different populations were considered to be shared if they both
501 overlapped with the same hotspot in the consensus set. To summarize all shared hotspots, a
502 Boolean matrix was constructed, in which a population having a hotspot that overlaps with
503 a hotspot in the consensus list leads to an indication of presence of the consensus hotspot
504 in that population. This matrix was used to determine hotspots shared by two or more
505 populations.

506 A Fisher's exact test was run for each pair of populations in order to determine whether
507 hotspots for the pair of populations overlap significantly more than expected. The BED
508 files containing the location of the recombination hotspots for each pair of populations were
509 compared using Bedtools:fisher (Quinlan and Hall, 2010). The number of comparisons was
510 45, making the the Bonferroni correction cutoff value: $\alpha = 0.0011$.

511 In order to compare the relationships between populations based on shared hotspots we
512 calculated Jaccard distances (`distance` function, `philentropy` package, R) (Drost, 2018)
513 and compared them to a published F_{ST} matrix (Cornejo et al., 2018) using a Mantel test
514 (`mantel.rtest` function, `ade4` package, R) (Chessel et al., 2004; Dray and Dufour, 2007;
515 Dray et al., 2007; Bougeard and Dray, 2018).

516 The Boolean matrix for shared hotspots was also used to explore the relationship be-
517 tween hotspot similarities and genetic covariances from a previous study (Cornejo et al.,
518 2018). Singletons were removed from the hotspot matrix, which was converted to a corre-
519 lation matrix using the `mixed.cor` function from the `psych` package in R (Revelle, 2018).
520 The `mixed.cor` function was used due to its ability to calculate Pearson correlations from
521 dichotomous data. We then used the `eigen` function in R (R Core Team, 2018) to generate
522 eigenvectors for the hotspot correlation matrix and the genetic covariance matrix. Pearson
523 correlations between the first and second eigenvector of the genetic covariance matrix and the
524 hotspot correlation matrix were then calculated (`cor.test` function, `stats` package, R)(R
525 Core Team, 2018). This analysis was done once with all populations included, and once with
526 the Criollo population excluded before correlations were calculated.

527 In order to model the presence or absence of hotspots along a drift tree, a multiple
528 correspondance analysis was used on the Boolean matrix of shared hotspots using the `MCA`
529 function from the `FactoMineR` package in R Lê et al. (2008). Nine dimensions were retained
530 and used as traits along a previously generated drift tree (Cornejo et al., 2018). Using the
531 `Rphylopars` package in R (Goolsby et al., 2016), the dimensions were modeled as Brownian
532 motion and as an Ornstein–Uhlenbeck process. The fit of the two models were compared
533 using the AIC values for the best fitting models of each type.

534

535 *Identifying DNA sequence motifs associated with the locations of recombination hotspots*

536

537 Motifs associated with hotspots were found using `RepeatMasker` (Smith et al., 2016).
538 The entire genome, the set of consensus hotspots, and a set of ubiquitous hotspots (hotspots
539 shared by at least eight of the populations) were examined with `RepeatMasker`, using normal
540 speed and "theobroma cacao" in the species option. In order to determine whether ubiqui-
541 tous hotspots were enriched for particular DNA sequences, a set of the same number and size

542 of sequences was randomly selected from the genome using Bedtools:shuffle (Quinlan and
543 Hall, 2010) and examined with RepeatMasker. This simulation was repeated one thousand
544 times and a null distribution against which observed values were compared was constructed
545 from the results.

546

547 *Identifying genomic features associated with the location of recombination hotspots*

548

549 Testing whether recombination hotspots were overrepresented near particular genomic
550 features was done by using a resampling scheme to establish null expectations and then
551 comparing the observed value to the empirical distribution. For each feature, locations were
552 retrieved and the number of observed hotspots that overlap with this feature were counted.
553 To determine whether this amount of overlapping hotspots was unusually high or low, a set of
554 hotspots that matched the number of hotspots and the size of each hotspot was simulated.
555 These simulated hotspots were placed randomly along the chromosome, using a uniform
556 distribution. The simulation was run 1000 times and the number of simulated hotspots that
557 overlap with the true genomic features was measured for each simulation. The simulations
558 generate an expected distribution of overlap with the genomic feature, and the true value
559 was then compared to the distribution. When simulated hotspots overlapped, the location
560 of one of them was sampled again. Features tested were: Transcriptional start sites (TSSs),
561 transcriptional termination sites (TTSs), exons, and introns. TSSs and TTSs are considered
562 to be the 500bp upstream and downstream of coding regions respectively.

563 The reason for the proposed novel resampling scheme is that, if the size and distribution
564 of genomic features and hotspots were not taken into account, it would set unrealistic expect-
565 ations for the overlap between features under a null model of no association. In this sense,
566 the null model would be inappropriate and potentially inflate the false positive rate.

567

568 *Data and code availability*

569

570 Rate and summary files from LDhat runs as well as hotspots for each population will be
571 placed in a Dryad repository (url). Scripts for LDhat and LDhot runs as well as additional
572 analysis is compiled in the following github repository *ejschwarzkopf/recombination-map*.

573

574 **Tables**

Population	Mean 4N _e r/kb	Mean N _e	Mean r/kb	Median r/kb	Lower Bound (Mean r/kb)	Upper Bound (Mean r/kb)	Mean cM/Mb
Amelonado	1.58	15744	2.51e-05	2.40e-09	2.48e-05	2.54e-05	4.04e-06
Contamana	8.53	61102	3.49e-05	4.92e-06	3.48e-05	3.50e-05	7.74e-05
Criollo	14.60	695	5.25e-03	4.27e-03	5.23e-03	5.27e-03	3.91e-03
Curaray	10.36	58213	4.45e-05	1.78e-05	4.44e-05	4.46e-05	1.18e-04
Guianna	8.66	4651	4.65e-04	7.74e-06	4.63e-04	4.67e-04	2.74e-04
Iquitos	4.23	49984	2.11e-05	5.88e-09	2.10e-05	2.12e-05	1.84e-05
Maranon	4.09	34037	3.01e-05	1.64e-08	2.99e-05	3.02e-05	1.68e-05
Nacional	4.66	26060	4.47e-05	9.76e-08	4.44e-05	4.49e-05	4.10e-05
Nanay	6.82	42429	4.02e-05	1.51e-07	4.00e-05	4.04e-05	1.33e-05
Purus	5.95	17357	8.57e-05	7.74e-06	8.54e-05	8.60e-05	1.23e-04

Table 1: Recombination rates in $4N_e r/kb$, r/kb , and cM/Mb for all ten *T. cacao* populations. The N_e that was used for the transformation is also reported for each population, as are the lower and upper bounds of a 95% confidence interval for r/kb .

575

Population	Ame	Con	Cri	Cur	Gui	Iqu	Mar	Nac	Nan
Amelonado	-	-	-	-	-	-	-	-	-
Contamana	<2e-07	-	-	-	-	-	-	-	-
Criollo	<9e-05	<5e-13	-	-	-	-	-	-	-
Curaray	<3e-05	<3e-37	<5e-08	-	-	-	-	-	-
Guianna	<3e-06	<1e-37	<7e-07	<4e-20	-	-	-	-	-
Iquitos	<4e-08	<6e-87	<2e-11	<3e-16	<2e-29	-	-	-	-
Maranon	<6e-13	<7e-77	<2e-11	<2e-20	<5e-33	<4e-64	-	-	-
Nacional	0.0015	<2e-43	0.0212	<7e-14	<3e-06	<6e-14	<3e-13	-	-
Nanay	0.0004	<2e-44	<9e-11	<4e-16	<2e-21	<3e-39	<2e-38	<9e-06	-
Purus	0.1782	<4e-117	<2e-05	<2e-29	<1e-33	<2e-39	<8e-43	<6e-27	<2e-21

Table 2: Fisher’s exact test p-values for pairwise comparisons of recombination hotspot locations between populations of *T. cacao*

576

577

Measures	Observed % ubiquitous HS	Observed % all HS	Observed % whole genome	Mean % Sim	% Sim >ubiquitous HS
Retroelements	2.34	9.45	11.12	11.11	99.9
DNA transposons	1.94	1.64	1.10	1.10	5.4
Total	4.28	11.09	12.21	12.22	99.7

Table 3: Percentage of DNA sequences identified as either retroelements or DNA transposons, and total interspersed repeats. Observed values for the entire *T. cacao* genome, for all recombination hotspots (HS), and ubiquitous hotspots (hotspots in the same location in at least eight different populations). Also presented are mean percentage of these sequences for 1000 simulations of hotspots equivalent in size and count as the ubiquitous set and the percentile at which the observed value for the ubiquitous set is found in the distribution of the simulated set (Sim).

	TSSs (500bp)	TTSs (500bp)	Exon	Intron
Amelonado	1	1	0.602	0.527
Contamana	1	1	0.000	0.000
Criollo	1	1	0.000	0.000
Curaray	1	1	0.346	0.058
Guianna	1	1	1.000	1.000
Iquitos	1	1	0.000	0.000
Maranon	1	1	0.000	0.000
Nacional	1	1	0.000	0.000
Nanay	1	1	0.027	0.237
Purus	1	1	0.004	0.000

Table 4: Proportion of simulated chromosomes that presented a lower amount of hotspots intersecting with TSSs, TTSs, exons, and introns. TSSs and TTSs are considered to be the 500bp upstream and downstream of coding regions, respectively.

578

579

580

Population	Mean Hotspot Size (kb)
Amelonado	6.9
Contamana	6.1
Criollo	6.1
Curaray	5.8
Guianna	8.6
Iquitos	7.0
Maranon	6.8
Nacional	6.9
Nanay	7.6
Purus	6.3
All hotspots	6.9

Table 5: Average hotspot size (in kb) for hotspots detected in each population and average for all hotspots.

Pop	Position L95	Position U95	Genome L95	Genome U95	Position Range Quotient	Genome Range Quotient
Amelonado	6.35e-10	7.67e-08	2.33e-10	3.13e-04	120.75	1.34e+06
Contamana	1.63e-06	1.34e-05	1.40e-09	2.64e-04	8.22	1.88e+05
Criollo	8.75e-04	4.31e-03	5.35e-07	1.66e-02	4.92	3.11e+04
Curaray	5.15e-06	2.63e-05	2.72e-09	2.02e-04	5.11	7.40e+04
Guianna	9.76e-06	1.26e-04	1.81e-09	2.96e-03	12.90	1.63e+06
Iquitos	3.50e-10	6.52e-08	1.58e-10	2.45e-04	186.29	1.55e+06
Maranon	1.98e-09	7.40e-07	2.31e-10	3.52e-04	373.35	1.52e+06
Nacional	4.80e-10	6.50e-08	2.76e-10	3.66e-04	135.60	1.33e+06
Nanay	1.65e-09	3.06e-07	2.06e-10	3.52e-04	185.32	1.71e+06
Purus	3.98e-08	5.24e-06	2.00e-09	6.35e-04	131.87	3.18e+05

Table 6: The median of the upper and lower bounds of the 95% Credibility Interval for the trace of estimates of r from all positions in the genome are presented for each population. The upper and lower bounds of the 95% probability interval for the median estimate of r for each population is also presented. The quotients of the upper and lower bounds for each interval point to a much larger genome-wide variation in r than per-position variation in the trace for the estimate of r .

581 **Figures**

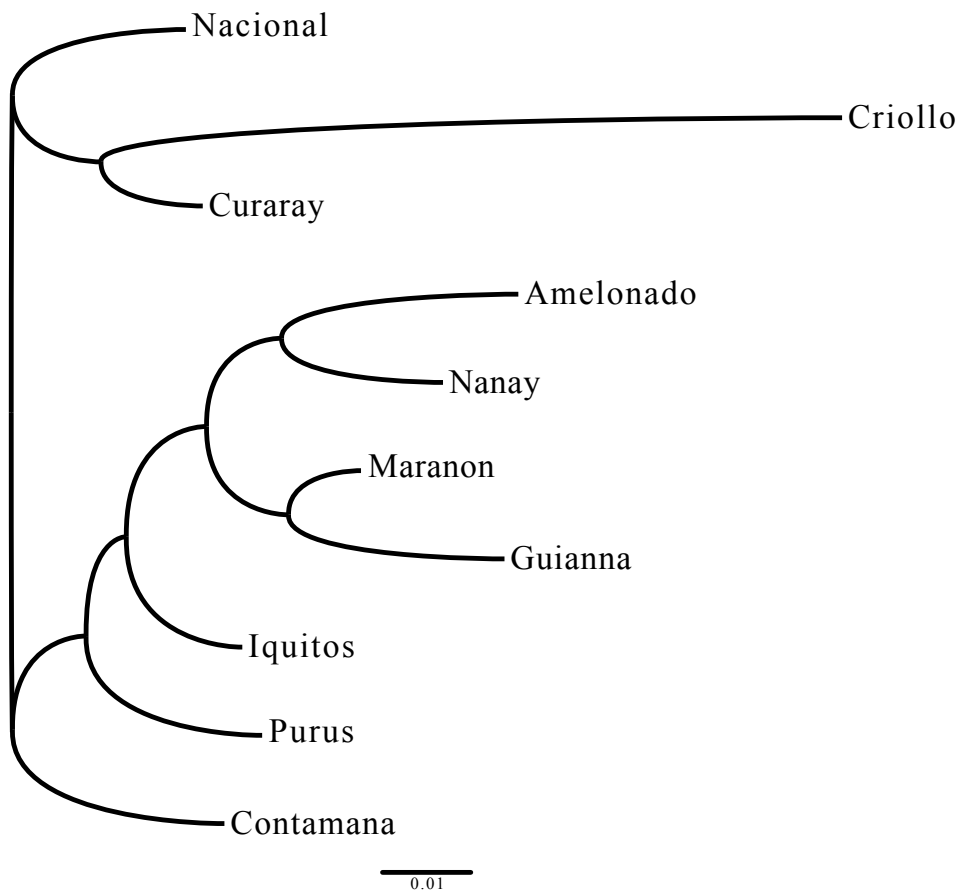


Figure 1: Drift tree for the 10 *T. cacao* populations. Modified from Cornejo et al. (2018)

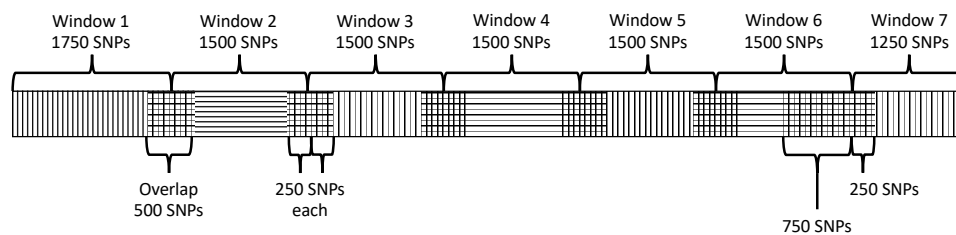


Figure 2: Example of the window layout for a 10,750 SNP chromosome. The 2,000 SNP long windows are represented by alternating horizontal and vertical lines and the overlaps between them are represented by square crosshatches. Braces above the chromosome indicate the regions from which recombination rates are extracted to generate the chromosome-wide recombination rates.

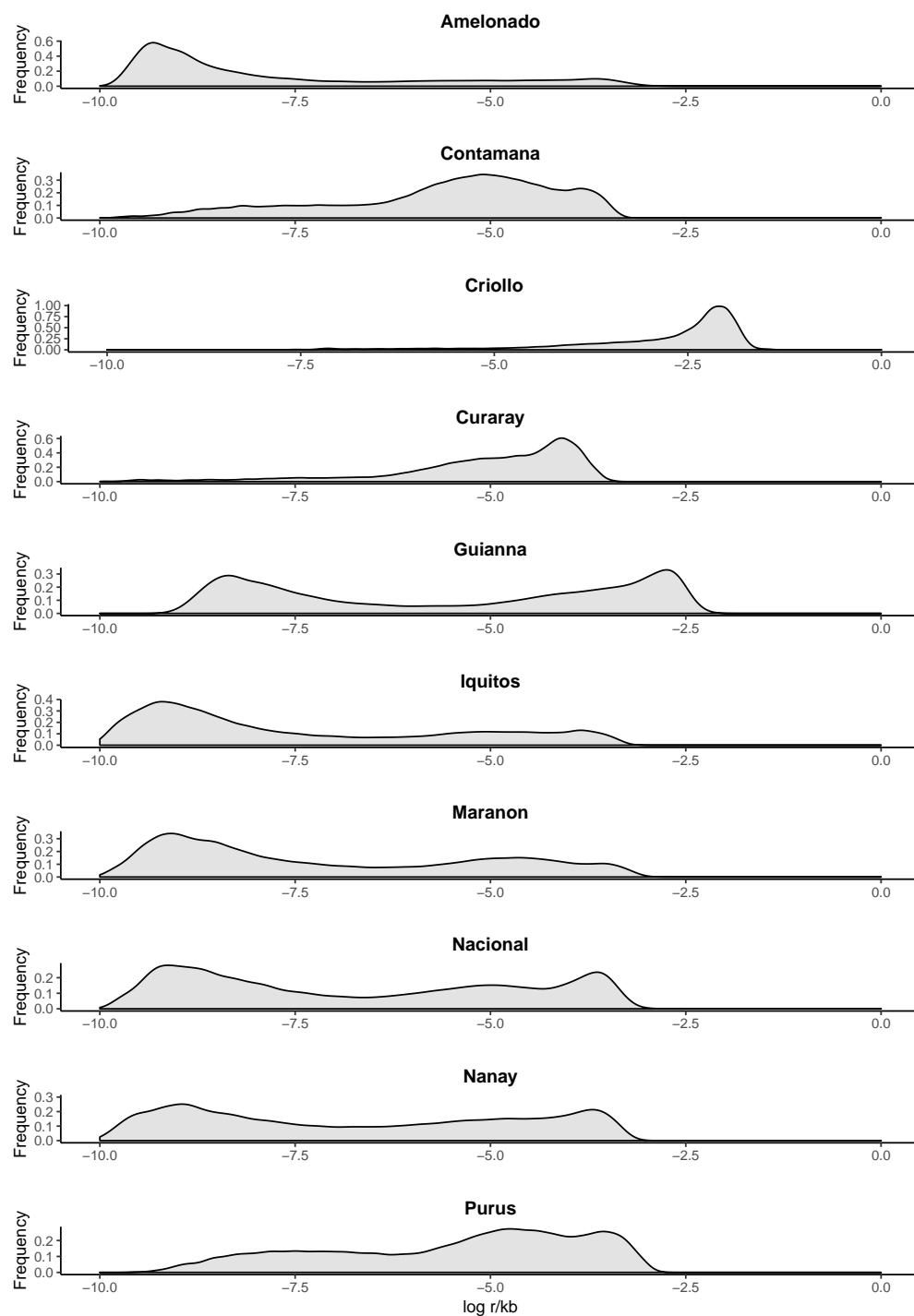


Figure 3: Distribution of \log_{10} recombination rates (r/kb) along the genomes of the ten *T. cacao* populations.

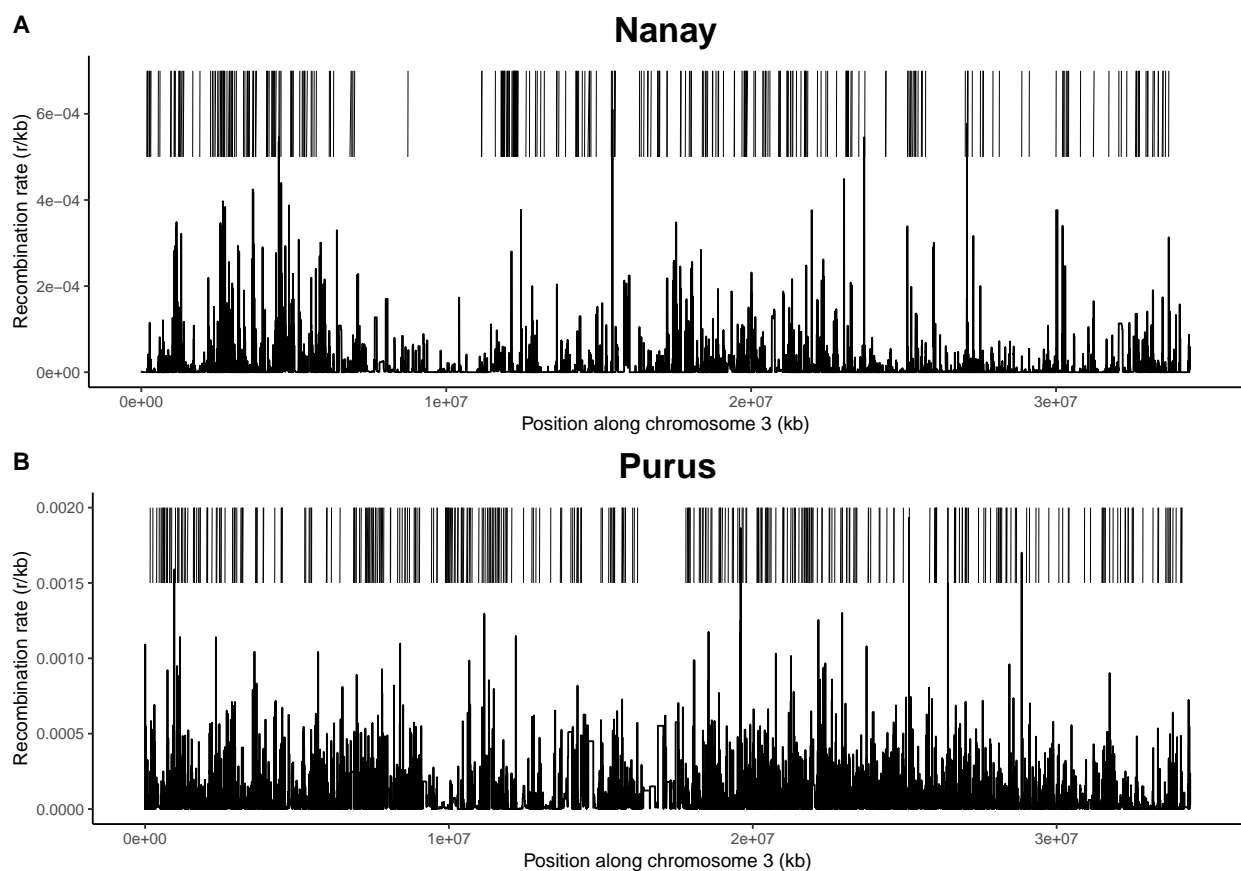


Figure 4: The third chromosomes of the Nanay (A) and Purus (B) populations were selected to exemplify the differences between populations in recombination rates (r/kb) and recombination hotspot locations (red vertical line segments).

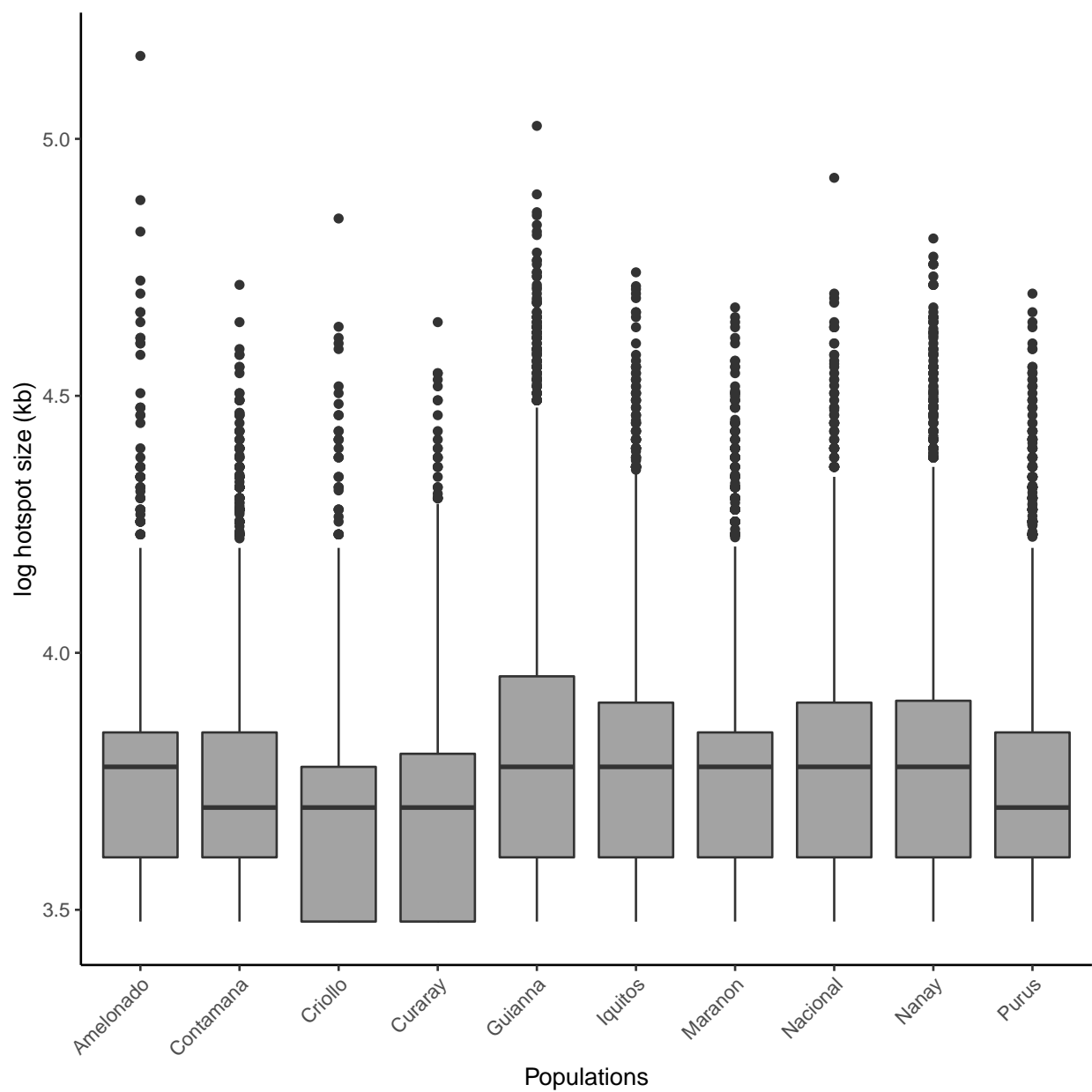


Figure 5: Boxplots of recombination hotspot sizes ($\log_{10}(kb)$) by population. The horizontal line in the box represents the median value, while the points represent potential outliers.

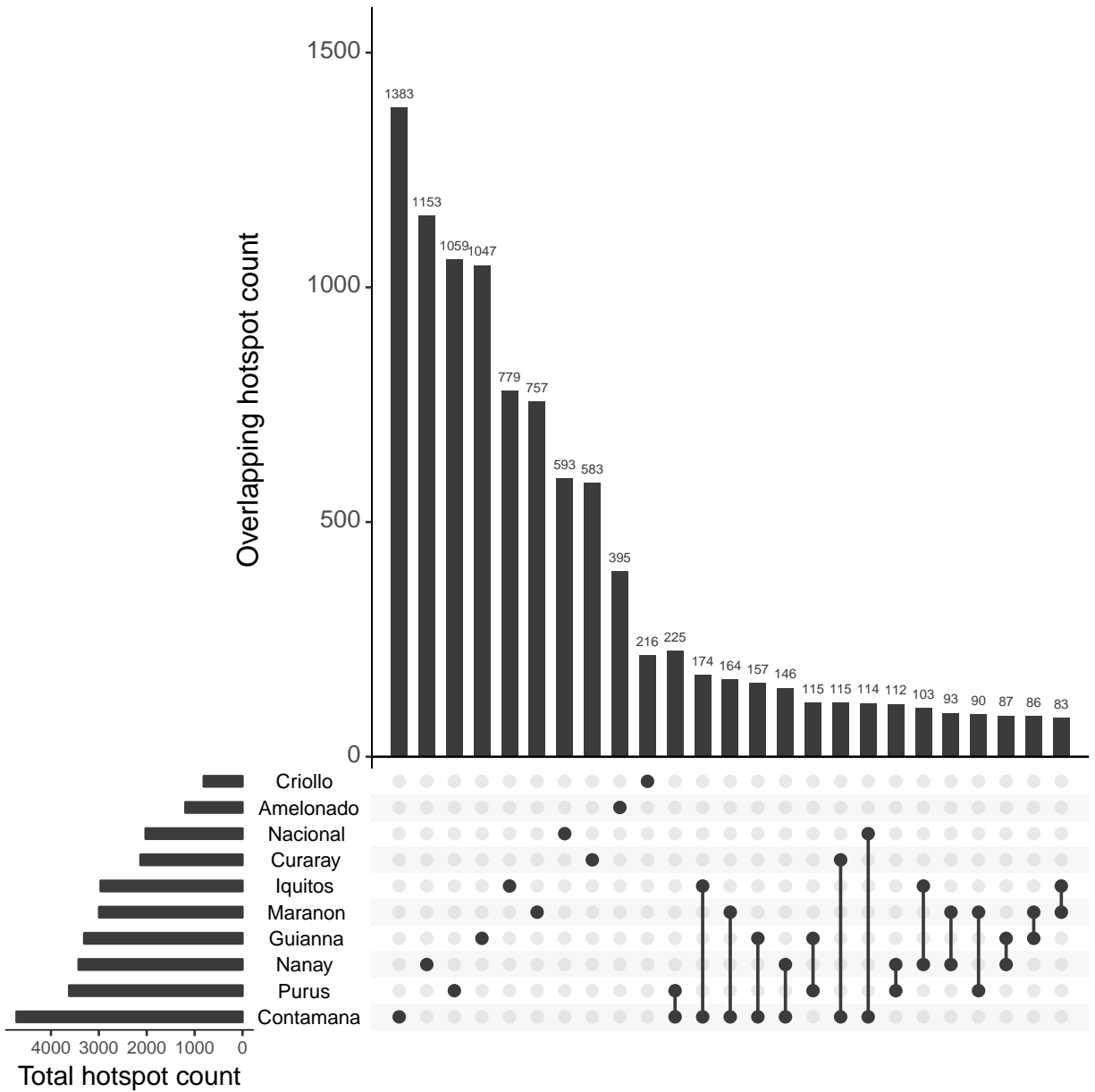


Figure 6: Upset plot showing amounts of shared hotspots. Horizontal bars represent total hotspots detected in a population, dots on the matrix represent the populations that share the hotspots represented in the vertical bar above them. The 25 largest subsets are shown.

582 References

- 583 Akhunov, E. D., and Coauthors, 2003: The organization and rate of evolution of wheat
584 genomes are correlated with recombination rates along chromosome arms. *Genome re-*
585 *search*, **13** (5).
- 586 Anderson, L. K., N. Salameh, H. W. Bass, L. C. Harper, W. Z. Cande, G. Weber, and S. M.
587 Stack, 2004: Integrating genetic linkage maps with pachytene chromosome structure in
588 maize. *Genetics*, **166** (4), 1923–1933, doi:10.1534/genetics.166.4.1923, URL [http://www.](http://www.genetics.org/content/166/4/1923)
589 [genetics.org/content/166/4/1923](http://www.genetics.org/content/166/4/1923), <http://www.genetics.org/content/166/4/1923.full.pdf>.
- 590 Auton, A., and G. McVean, 2007: Recombination rate estimation in the presence of hotspots.
591 *Genome Research*, **17** (8), 1219–1227, URL [http://www.ncbi.nlm.nih.gov/pmc/articles/](http://www.ncbi.nlm.nih.gov/pmc/articles/PMC1933511/)
592 [PMC1933511/](http://www.ncbi.nlm.nih.gov/pmc/articles/PMC1933511/).
- 593 Auton, A., and Coauthors, 2012: A Fine-Scale Chimpanzee Genetic Map from Popula-
594 tion Sequencing. *Science*, **336** (6078), 193–198, doi:10.1126/science.1216872, URL [http:](http://science.sciencemag.org/content/336/6078/193)
595 [//science.sciencemag.org/content/336/6078/193](http://science.sciencemag.org/content/336/6078/193), [http://science.sciencemag.org/content/](http://science.sciencemag.org/content/336/6078/193.full.pdf)
596 [336/6078/193.full.pdf](http://science.sciencemag.org/content/336/6078/193.full.pdf).
- 597 Auton, A., and Coauthors, 2013: Genetic recombination is targeted towards gene promoter
598 regions in dogs. *PLOS Genetics*, **9** (12), 1–9, doi:10.1371/journal.pgen.1003984, URL
599 <https://doi.org/10.1371/journal.pgen.1003984>.
- 600 Bartley, B., 2005: *The Genetic Diversity of Cacao and Its Utilization*. CAB books, CABI,
601 URL https://books.google.com/books?id=_I40iGVJD64C.
- 602 Begun, D. J., and C. F. Aquadro, 1992: Levels of naturally occurring dna polymorphism
603 correlate with recombination rates in *d. melanogaster*. *Nature*, **356** (6369).

- 604 Booker, T. R., R. W. Ness, and P. D. Keightley, 2017: The recombination landscape in
605 wild house mice inferred using population genomic data. *Genetics*, **207** (1), 297–309,
606 doi:10.1534/genetics.117.300063, URL <http://www.genetics.org/content/207/1/297>, <http://www.genetics.org/content/207/1/297.full.pdf>.
- 608 Bougeard, S., and S. Dray, 2018: Supervised multiblock analysis in R with the ade4 package.
609 *Journal of Statistical Software*, **86** (1), 1–17, doi:10.18637/jss.v086.i01.
- 610 Branca, A., and Coauthors, 2011: Whole-genome nucleotide diversity, recombination, and
611 linkage disequilibrium in the model legume *medicago truncatula*. *Proceedings of the Na-*
612 *tional Academy of Sciences*, **108** (42).
- 613 Brick Kevin, Smagulova Fatima, Khil Pavel, Camerini-Otero R. Daniel, and Petukhova
614 Galina V., 2012: Genetic recombination is directed away from functional ge-
615 nomic elements in mice. *Nature*, **485** (7400), 642–645, doi:[http://dx.doi.org/](http://dx.doi.org/10.1038/nature11089)
616 [10.1038/nature11089](http://dx.doi.org/10.1038/nature11089), URL [http://www.nature.com/nature/journal/v485/n7400/abs/](http://www.nature.com/nature/journal/v485/n7400/abs/nature11089.html#supplementary-information)
617 [nature11089.html#supplementary-information](http://www.nature.com/nature/journal/v485/n7400/abs/nature11089.html#supplementary-information), [10.1038/nature11089](http://dx.doi.org/10.1038/nature11089).
- 618 Brunschwig, H., L. Levi, E. Ben-David, R. W. Williams, B. Yakir, and S. Shifman, 2012:
619 Fine-scale Map of Recombination Rates and Hotspots in the Mouse Genome. *Genet-*
620 *ics*, doi:10.1534/genetics.112.141036, URL [http://www.genetics.org/content/early/2012/](http://www.genetics.org/content/early/2012/05/04/genetics.112.141036)
621 [05/04/genetics.112.141036](http://www.genetics.org/content/early/2012/05/04/genetics.112.141036), [http://www.genetics.org/content/early/2012/05/04/genetics.](http://www.genetics.org/content/early/2012/05/04/genetics.112.141036.full.pdf)
622 [112.141036.full.pdf](http://www.genetics.org/content/early/2012/05/04/genetics.112.141036.full.pdf).
- 623 Chen, M.-M., F. Feng, X. Sui, M.-H. Li, D. Zhao, and S. Han, 2010: Construction of
624 a framework map for *pinus koraiensis sieb. et zucc.* using srp, ssr and issr markers.
625 *Trees*, **24** (4), 685–693, doi:10.1007/s00468-010-0438-5, URL [https://doi.org/10.1007/](https://doi.org/10.1007/s00468-010-0438-5)
626 [s00468-010-0438-5](https://doi.org/10.1007/s00468-010-0438-5).

- 627 Chessel, D., A.-B. Dufour, and J. Thioulouse, 2004: The ade4 package – I: One-table meth-
628 ods. *R News*, **4** (1), 5–10, URL <https://cran.r-project.org/doc/Rnews/>.
- 629 Choi, K., and Coauthors, 2013: *Arabidopsis* meiotic crossover hot spots overlap with
630 h2a.z nucleosomes at gene promoters. *Nature Genetics*, **45** (11), 1327–1336, doi:
631 10.1038/ng.2766.
- 632 Cornejo, O. E., and Coauthors, 2018: Population genomic analyses of the chocolate tree,
633 *Theobroma cacao* L., provide insights into its domestication process. *Communications*
634 *Biology*, doi:10.1038/s42003-018-0168-6.
- 635 Crow, J. F. J. F., 1970: (Harper international editions.). An introduction to population
636 genetics theory. Harper Row, New York.
- 637 Danecek Petr, and Coauthors, 2011: The variant call format and VCFtools. *Bioinformatics*,
638 **27** (15), 2156–2158, URL <http://www.ncbi.nlm.nih.gov/pmc/articles/PMC3137218/>.
- 639 Donnelly, P., and T. G. Kurtz, 1999: Genealogical processes for fleming-viot models with
640 selection and recombination. *Ann. Appl. Probab.*, **9** (4), 1091–1148, doi:10.1214/aoap/
641 1029962866, URL <https://doi.org/10.1214/aoap/1029962866>.
- 642 Dray, S., and A.-B. Dufour, 2007: The ade4 package: Implementing the duality diagram for
643 ecologists. *Journal of Statistical Software*, **22** (4), 1–20, doi:10.18637/jss.v022.i04.
- 644 Dray, S., A.-B. Dufour, and D. Chessel, 2007: The ade4 package – II: Two-table and K-table
645 methods. *R News*, **7** (2), 47–52, URL <https://cran.r-project.org/doc/Rnews/>.
- 646 Drost, H.-G., 2018: *philentropy: Similarity and Distance Quantification Between Probabil-*
647 *ity Functions*. URL <https://CRAN.R-project.org/package=philentropy>, r package version
648 0.2.0.

- 649 Exposito-Alonso, M., and Coauthors, 2018: The rate and potential relevance of new mu-
650 tations in a colonizing plant lineage. *PLOS Genetics*, **14** (2), 1–21, doi:10.1371/journal.
651 pgen.1007155, URL <https://doi.org/10.1371/journal.pgen.1007155>.
- 652 Eyre-Walker, A., and P. D. Keightley, 2007: The distribution of fitness effects of new muta-
653 tions. *Nature Reviews Genetics*, **8** (8).
- 654 Felsenstein, J., 1974: The evolutionary advantage of recombination. *Genetics*, **78** (2),
655 737–756, URL <http://www.genetics.org/content/78/2/737>, [http://www.genetics.org/
656 content/78/2/737.full.pdf](http://www.genetics.org/content/78/2/737.full.pdf).
- 657 Fernandes, J. B., M. Séguéla-Arnaud, C. Larchevêque, A. H. Lloyd, and R. Mercier, 2018:
658 Unleashing meiotic crossovers in hybrid plants. *Proceedings of the National Academy of Sci-*
659 *ences*, **115** (10), 2431–2436, doi:10.1073/pnas.1713078114, URL [http://www.pnas.org/
660 content/115/10/2431](http://www.pnas.org/content/115/10/2431), <http://www.pnas.org/content/115/10/2431.full.pdf>.
- 661 Goolsby, E. W., J. Bruggeman, and C. Ane, 2016: *Rphylopars: Phylogenetic Comparative*
662 *Tools for Missing Data and Within-Species Variation*. URL [https://CRAN.R-project.org/
663 package=Rphylopars](https://CRAN.R-project.org/package=Rphylopars), r package version 0.2.9.
- 664 Gore, M. A., and Coauthors, 2009: A first-generation haplotype map of maize. *Science*,
665 **326** (5956), 1115–1117, doi:10.1126/science.1177837, URL [http://science.sciencemag.
666 org/content/326/5956/1115](http://science.sciencemag.org/content/326/5956/1115), [http://science.sciencemag.org/content/326/5956/1115.full.
667 pdf](http://science.sciencemag.org/content/326/5956/1115.full.pdf).
- 668 Haldane, J. B. S., 1937: The effect of variation on fitness. *The American Naturalist*, **71** (735),
669 337–349, URL <http://www.jstor.org/stable/2457289>.
- 670 Hellsten, U., and Coauthors, 2013: Fine-scale variation in meiotic recombination in
671 *Mimulus* inferred from population shotgun sequencing. *PNAS*, **110** (48), 19478–19482,
672 doi:10.1073/pnas.1319032110.

- 673 Henderson, J. S., R. A. Joyce, G. R. Hall, W. J. Hurst, and P. E. McGovern, 2007: Chemical
674 and archaeological evidence for the earliest cacao beverages. *Proceedings of the National*
675 *Academy of Sciences*, **104** (48), 18 937–18 940, doi:10.1073/pnas.0708815104, URL [http:](http://www.pnas.org/content/104/48/18937.abstract)
676 [//www.pnas.org/content/104/48/18937.abstract](http://www.pnas.org/content/104/48/18937.abstract), [http://www.pnas.org/content/104/48/](http://www.pnas.org/content/104/48/18937.full.pdf)
677 [18937.full.pdf](http://www.pnas.org/content/104/48/18937.full.pdf).
- 678 Hudson, R. R., and N. L. Kaplan, 1988: The coalescent process in models with selection and
679 recombination. *Genetics*, **120** (3), 831–840, URL [http://www.genetics.org/content/120/](http://www.genetics.org/content/120/3/831)
680 [3/831](http://www.genetics.org/content/120/3/831), <http://www.genetics.org/content/120/3/831.full.pdf>.
- 681 Kim, S., and Coauthors, 2007: Recombination and linkage disequilibrium in arabidopsis
682 thaliana. *Nature Genetics*, **39** (9).
- 683 Kosambi, D. D., 1943: The estimation of map distances from recombination val-
684 ues. *Annals of Eugenics*, **12** (1), 172–175, doi:10.1111/j.1469-1809.1943.tb02321.x,
685 URL <https://onlinelibrary.wiley.com/doi/abs/10.1111/j.1469-1809.1943.tb02321.x>, [https:](https://onlinelibrary.wiley.com/doi/pdf/10.1111/j.1469-1809.1943.tb02321.x)
686 [//onlinelibrary.wiley.com/doi/pdf/10.1111/j.1469-1809.1943.tb02321.x](https://onlinelibrary.wiley.com/doi/pdf/10.1111/j.1469-1809.1943.tb02321.x).
- 687 Kundu, A., A. Chakraborty, N. A. Mandal, D. Das, P. G. Karmakar, N. K. Singh, and
688 D. Sarkar, 2015: A restriction-site-associated dna (rad) linkage map, comparative genomics
689 and identification of qtl for histological fibre content coincident with those for retted
690 bast fibre yield and its major components in jute (*corchorus olitorius* l., malvaceae s. l.).
691 *Molecular Breeding*, **35** (1), 19, doi:10.1007/s11032-015-0249-x, URL [https://doi.org/10.](https://doi.org/10.1007/s11032-015-0249-x)
692 [1007/s11032-015-0249-x](https://doi.org/10.1007/s11032-015-0249-x).
- 693 Lê, S., J. Josse, and F. Husson, 2008: FactoMineR: A package for multivariate analysis.
694 *Journal of Statistical Software*, **25** (1), 1–18, doi:10.18637/jss.v025.i01.
- 695 Li, W. H., and M. Nei, 1974: Stable linkage disequilibrium without epistasis in subdivided
696 populations. *Theoretical population biology.*, **6** (2), 173–183.

- 697 Lynch, M., 2010: Evolution of the mutation rate. *Trends in genetics : TIG*, **26 (8)**, 345–352,
698 URL <http://www.ncbi.nlm.nih.gov/pmc/articles/PMC2910838/>.
- 699 Martinez-perez, E., M. Schvarzstein, C. Barroso, J. M. Lightfoot, A. F. Dernburg, and A. M.
700 Villeneuve, 2008: Crossovers trigger a remodeling of meiotic chromosome axis composition
701 that is linked to two-step loss of sister chromatid cohesion. *Genes & development*, **22 20**,
702 2886–901.
- 703 Mcvean, G., 2010: What drives recombination hotspots to repeat dna in humans? *Philo-*
704 *sophical Transactions of the Royal Society B*, **365 (1544)**, 1213–1218.
- 705 McVean, G. A. T., S. R. Myers, S. Hunt, P. Deloukas, D. R. Bentley, and P. Donnelly, 2004:
706 The fine-scale structure of recombination rate variation in the human genome. *Science*,
707 **304 (5670)**, 581–584, doi:10.1126/science.1092500, URL [http://science.sciencemag.org/](http://science.sciencemag.org/content/304/5670/581)
708 [content/304/5670/581](http://science.sciencemag.org/content/304/5670/581), <http://science.sciencemag.org/content/304/5670/581.full.pdf>.
- 709 Mézard, C., 2006: Meiotic recombination hotspots in plants. *Biochemical Society Transac-*
710 *tions*, **34 (4)**, 531–534, doi:10.1042/BST0340531, URL [http://www.biochemsoctrans.org/](http://www.biochemsoctrans.org/content/34/4/531)
711 [content/34/4/531](http://www.biochemsoctrans.org/content/34/4/531), <http://www.biochemsoctrans.org/content/34/4/531.full.pdf>.
- 712 Motamayor, J. C., P. Lachenaud, da Silva e Mota Jay Wallace, R. Loor, D. N. Kuhn, S. J.
713 Brown, and R. J. Schnell, 2008: Geographic and Genetic Population Differentiation of
714 the Amazonian Chocolate Tree (*Theobroma cacao* L). *PLOS ONE*, **3 (10)**, e3311, doi:
715 <https://doi.org/10.1371/journal.pone.0003311>.
- 716 Motamayor, J. C., and Coauthors, 2013: The genome sequence of the most widely
717 cultivated cacao type and its use to identify candidate genes regulating pod color.
718 *Genome Biology*, **14 (6)**, r53, doi:10.1186/gb-2013-14-6-r53, URL [https://doi.org/10.](https://doi.org/10.1186/gb-2013-14-6-r53)
719 [1186/gb-2013-14-6-r53](https://doi.org/10.1186/gb-2013-14-6-r53).

- 720 Myers, S., L. Bottolo, C. Freeman, G. McVean, and P. Donnelly, 2005: A Fine-Scale Map
721 of Recombination Rates and Hotspots Across the Human Genome. *Science*, **310** (5746),
722 321–324, doi:10.1126/science.1117196, URL [http://science.sciencemag.org/content/310/](http://science.sciencemag.org/content/310/5746/321)
723 [5746/321](http://science.sciencemag.org/content/310/5746/321.full.pdf), <http://science.sciencemag.org/content/310/5746/321.full.pdf>.
- 724 Ohta, T., 1982: Linkage disequilibrium due to random genetic drift in finite subdivi-
725 ded populations. *Proceedings of the National Academy of Sciences*, **79** (6), 1940–
726 1944, doi:10.1073/pnas.79.6.1940, URL <http://www.pnas.org/content/79/6/1940>, <http://www.pnas.org/content/79/6/1940.full.pdf>.
- 728 Paape, T., P. Zhou, A. Branca, R. Briskine, N. Young, and P. Tiffin, 2012: Fine-Scale
729 Population Recombination Rates, Hotspots, and Correlates of Recombination in the
730 *Medicago truncatula* Genome. *Genome Biology and Evolution*, **4** (5), 726–737, URL
731 <http://www.ncbi.nlm.nih.gov/pmc/articles/PMC3381680/>.
- 732 Quinlan, A. R., and I. M. Hall, 2010: Bedtools: a flexible suite of utilities for comparing
733 genomic features. *Bioinformatics*, **26** (6), 841–842, doi:10.1093/bioinformatics/btq033,
734 URL [+http://dx.doi.org/10.1093/bioinformatics/btq033](http://dx.doi.org/10.1093/bioinformatics/btq033), [/oup/backfile/content_public/](http://oup/backfile/content_public/journal/bioinformatics/26/6/10.1093_bioinformatics_btq033/3/btq033.pdf)
735 [journal/bioinformatics/26/6/10.1093_bioinformatics_btq033/3/btq033.pdf](http://oup/backfile/content_public/journal/bioinformatics/26/6/10.1093_bioinformatics_btq033/3/btq033.pdf).
- 736 R Core Team, 2018: *R: A Language and Environment for Statistical Computing*. Vienna,
737 Austria, R Foundation for Statistical Computing, URL <https://www.R-project.org/>.
- 738 Revelle, W., 2018: *psych: Procedures for Psychological, Psychometric, and Personality Re-*
739 *search*. Evanston, Illinois, Northwestern University, URL [https://CRAN.R-project.org/](https://CRAN.R-project.org/package=psych)
740 [package=psych](https://CRAN.R-project.org/package=psych), r package version 1.8.10.
- 741 Rizzon, C., G. Marais, M. Gouy, and C. Biéumont, 2002: Recombination rate and the distri-
742 bution of transposable elements in the *drosophila melanogaster* genome. *Genome Research*,

- 743 **12 (3)**, 400–407, doi:10.1101/gr.210802, URL <http://genome.cshlp.org/content/12/3/400>.
744 abstract, <http://genome.cshlp.org/content/12/3/400.full.pdf+html>.
- 745 Rodgers, K., and M. Mcvey, 2015: Error-prone repair of dna double-strand breaks. *Journal*
746 *of Cellular Physiology*, **231**.
- 747 Ross-Ibarra, J., 2004: The Evolution of Recombination under Domestication: A Test of
748 Two Hypotheses. *The American Naturalist*, **163 (1)**, 105–112, doi:10.1086/380606, URL
749 <https://doi.org/10.1086/380606>, PMID: 14767840, <https://doi.org/10.1086/380606>.
- 750 Sanjuán, R., A. Moya, and S. F. Elena, 2004: The distribution of fitness effects caused
751 by single-nucleotide substitutions in an rna virus. *Proceedings of the National Academy*
752 *of Sciences*, **101 (22)**, 8396–8401, doi:10.1073/pnas.0400146101, URL <http://www.pnas.org/content/101/22/8396>,
753 <http://www.pnas.org/content/101/22/8396.full.pdf>.
- 754 Schnable, P. S., and Coauthors, 2009: The b73 maize genome: complexity, diversity, and
755 dynamics. *Science (New York, N.Y.)*, **326 (5956)**.
- 756 Shanfelter, A., S. L. Archambeault, and M. A. White, 2018: Fine-scale recombination
757 landscapes between a freshwater and marine population of threespine stickleback fish.
758 *bioRxiv*, doi:10.1101/430249, URL [https://www.biorxiv.org/content/early/2018/09/29/](https://www.biorxiv.org/content/early/2018/09/29/430249)
759 [430249, https://www.biorxiv.org/content/early/2018/09/29/430249.full.pdf](https://www.biorxiv.org/content/early/2018/09/29/430249.full.pdf).
- 760 Singhal, S., and Coauthors, 2015: Stable recombination hotspots in birds. *Science*,
761 **350 (6263)**, 928–932, doi:10.1126/science.aad0843, URL [http://science.sciencemag.org/](http://science.sciencemag.org/content/350/6263/928)
762 [content/350/6263/928, http://science.sciencemag.org/content/350/6263/928.full.pdf](http://science.sciencemag.org/content/350/6263/928.full.pdf).
- 763 Siol, M., I. Bonnin, I. Oliveri, J. M. Prospero, and J. Ronfort, 2007: Effective population
764 size associated with self-fertilization: lessons from temporal changes in allele frequencies
765 in the selfing annual medicago truncatula. *Journal of Evolutionary Biology*, **20 (6)**, 2349–
766 2360, doi:10.1111/j.1420-9101.2007.01409.x, URL <https://onlinelibrary.wiley.com/doi/>

767 [abs/10.1111/j.1420-9101.2007.01409.x](https://doi.org/10.1111/j.1420-9101.2007.01409.x), [https://onlinelibrary.wiley.com/doi/pdf/10.1111/](https://onlinelibrary.wiley.com/doi/pdf/10.1111/j.1420-9101.2007.01409.x)
768 [j.1420-9101.2007.01409.x](https://onlinelibrary.wiley.com/doi/pdf/10.1111/j.1420-9101.2007.01409.x).

769 Smith, A., R. Hubley, and P. Green, 2016: Repeatmasker open-4.0.(2013-2015).

770 Stapley, J., P. G. D. Feulner, S. E. Johnston, A. W. Santure, and C. M. Smadja, 2017: Vari-
771 ation in recombination frequency and distribution across eukaryotes: patterns and pro-
772 cesses. *Philosophical Transactions of the Royal Society B: Biological Sciences*, **372** (1736),
773 doi:10.1098/rstb.2016.0455, URL [http://rstb.royalsocietypublishing.org/content/372/](http://rstb.royalsocietypublishing.org/content/372/1736/20160455)
774 [1736/20160455](http://rstb.royalsocietypublishing.org/content/372/1736/20160455), [http://rstb.royalsocietypublishing.org/content/372/1736/20160455.full.](http://rstb.royalsocietypublishing.org/content/372/1736/20160455.full.pdf)
775 [pdf](http://rstb.royalsocietypublishing.org/content/372/1736/20160455.full.pdf).

776 Stevison, L. S., and Coauthors, 2016: The time scale of recombination rate evolution in great
777 apes. *Molecular Biology and Evolution*, **33** (4), 928–945, doi:10.1093/molbev/msv331.

778 Wloch, D. M., K. Szafraniec, R. H. Borts, and R. Korona, 2001: Direct estimate of the
779 mutation rate and the distribution of fitness effects in the yeast *saccharomyces cerevisiae*.
780 *Genetics*, **159** (2), 441–452, URL <http://www.genetics.org/content/159/2/441>, [http://](http://www.genetics.org/content/159/2/441.full.pdf)
781 www.genetics.org/content/159/2/441.full.pdf.

782 Wu, J., and Coauthors, 2003: Physical maps and recombination frequency of six rice chro-
783 mosomes. *Plant Journal*, **36** (5), 720–730.

784 Yelina, N., P. Diaz, C. Lambing, and I. R. Henderson, 2015: Epigenetic control of
785 meiotic recombination in plants. *Science China Life Sciences*, **58** (3), 223–231, doi:
786 [10.1007/s11427-015-4811-x](https://doi.org/10.1007/s11427-015-4811-x), URL <https://doi.org/10.1007/s11427-015-4811-x>.